Non-Slender Single Angle Struts

M. ELGAALY, W. DAVIDS and H. DAGHER

INTRODUCTION

A literature search indicated a lack of test results regarding non-slender single angle struts. The primary objective of this paper is to present and discuss the results of the tests conducted by the authors on non-slender single angle compression members. These angle members have equal legs and were tested to failure as part of a three-dimensional truss.

The paper briefly describes the authors' experimental program. The method of calculation of the member forces from the strain readings is discussed. The test results are given and six failure modes are identified. These failure modes depend on the member slenderness ratio, the angle leg width/thickness ratio, the end connection detail, and the eccentricity of the applied load. These failure modes can be generally classified as global with no appreciable local failures or local failures which triggered global failures in some cases.

Finally, the design rules given by the AISC Specification for Structural Steel Buildings[1–3] and the ASCE Manual 52 for the Design of Steel Transmission Towers[4] are evaluated.

EXPERIMENTAL PROGRAM

The number of tests on slender members is sufficient to permit accurate recommendations for design. However, there is not enough data to allow accurate design recommendations for non-slender members. In addition, many of the published tests do not reflect actual end conditions. The testing program conducted by the authors directly addresses the lack of data regarding non-slender single angle struts, while attempting to model actual end conditions as closely as possible.

Test Specimens: Fifty single-angle members, with equal legs, were tested as part of a truss. The tests included single and double bolted end connections. The selection of member sizes was based on the capacity of the truss and the need to cover a slenderness ratio range from 60 to 120. Table 1 lists the characteristics and numbers of the test specimens chosen.

Test Apparatus and Instrumentation: The three-dimensional truss used to test each specimen is shown in Figs. 1 and 2. The truss was designed so that the "target angle" would fail first without introducing significant deformations in the remainder of the truss. Following each test, only the target angle was replaced, allowing multiple tests to be conducted in the same setting. Load was applied via two 100 kip capacity hydraulic jacks which allowed the load on each side of the truss to be kept balanced. Each specimen was monitored with eight linear strain gages and displacements were measured in two orthogonal directions at the center of the specimens. In addition, each hydraulic jack had a corresponding load cell and digital readout to allow visual monitoring of the load during the test. All data was recorded by a computer except for the load cell readings which were taken manually. The eight strain gages were located in pairs to account for differential strains through the leg thickness as shown in Fig. 3. The displacement transducers were located as shown in Fig. 4. Transducers 1 and 2 monitored the movement of the center of the specimen relative to the reaction frame, and transducers 3 and 4 measured the movement of the top and bottom joints of the specimen relative to the reaction frame. Based on the four displacement readings, the displacements at the center of the specimen in two orthogonal directions can be determined. It should be noted that it was assumed that the truss did not deform out-of-plane and no provisions were made to measure the torsional rotation at the center of the angle.

Calculation of Member Forces from Strain Readings: The method used to calculate member forces from strain readings involves numerical integration of the stress over the crosssectional area and was developed to handle the inelastic failures encountered for the specimens tested. An advantage of this method is that it easily allows the inclusion of residual stresses in the analysis. This is accomplished by combining

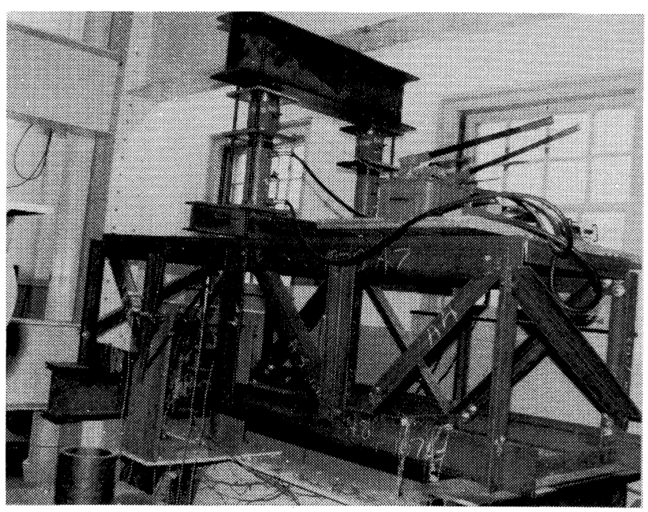

Fig. 1. Picture of truss.

M. Elgaaly is professor, W. Davids is graduate assistant, and H. Dagher is associate professor at the University of Maine, Orono, ME.

Table 1. Test Specimens				
Group	Size	L/r	End Conditions	Test Nos.
1	$1\frac{3}{4} \times 1\frac{3}{4} \times \frac{1}{8}$	98	double bolt	1, 2, 3, 4, 5
2	$1\frac{3}{4} \times 1\frac{3}{4} \times \frac{3}{16}$	99	double bolt	6, 7, 8, 33, 35
3	$2 \times 2 \times \frac{1}{8}$	85	double bolt	9, 10, 11, 12, 13
4	$2 \times 2 \times \frac{3}{16}$	86	double bolt	20, 21, 22, 43, 44
5	$2\frac{1}{2} \times 2\frac{1}{2} \times \frac{3}{16}$	87	double bolt	18, 19, 50, 51, 52
6	$1\frac{3}{4} \times 1\frac{3}{4} \times \frac{1}{8}$	92	single bolt	53, 54, 55, 56, 57
7	$1\frac{3}{4} \times 1\frac{3}{4} \times \frac{3}{16}$	93	single bolt	23, 24, 35, 36, 37
8	$2 \times 2 \times \frac{1}{8}$	80	single bolt	26, 27, 28, 38, 39
9	$2 \times 2 \times \frac{3}{16}$	81	single bolt	29, 31, 40, 41, 42
10	$2\frac{1}{2} \times 2\frac{1}{2} \times \frac{3}{16}$	65	single bolt	45, 46, 47, 48, 49

the residual stress diagram with the stress distribution calculated from the measured strains, and using elastic-perfectly-plastic material properties. The residual stress distribution shown in Fig. 5 was assumed. A sensitivity analysis was performed where the maximum value of the residual stress was varied from 0 to $0.3F_y$ where F_y is the actual yield stress of the specimen. It was found that the effect on the calculated axial force was on the order of five percent or less for most of the specimens tested. To provide a check on the accuracy of the axial force calculated as described above, two compression tests were conducted in a Baldwin testing machine. The ends were bolted in the same manner as the specimens tested in the truss, and eight strain gages were mounted on both angles. For each test, the calculated axial load was compared with the actual applied load which was read directly from the machine load indicator. The calculated failure load was two percent below the actual applied load in one case and was seven percent below the actual applied load in the other. Both of these values are within the range of experimental error.

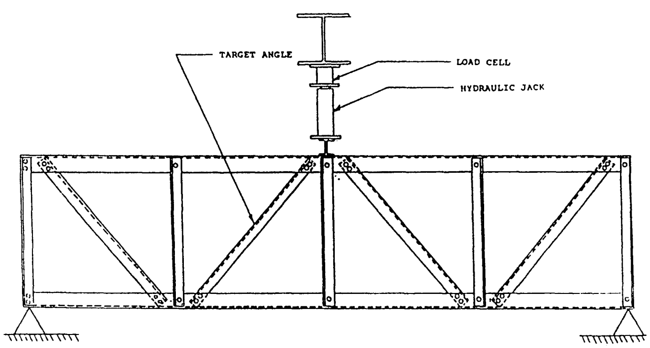

Fig. 2. Location of target angle.

EXPERIMENTAL RESULTS

The failure loads and the observed failure modes will be discussed. For the purpose of presenting and discussing the results, the tests have been grouped into ten categories as shown in Table 1.

Failure Modes: The first failure mode involves local buckling of the connected leg. This local buckling is coupled with torsional buckling or followed by flexural buckling about

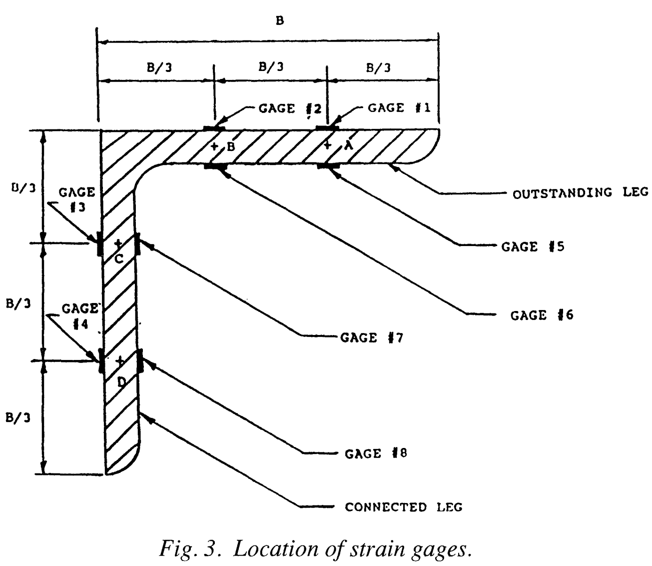

Fig. 3. Location of strain gages.

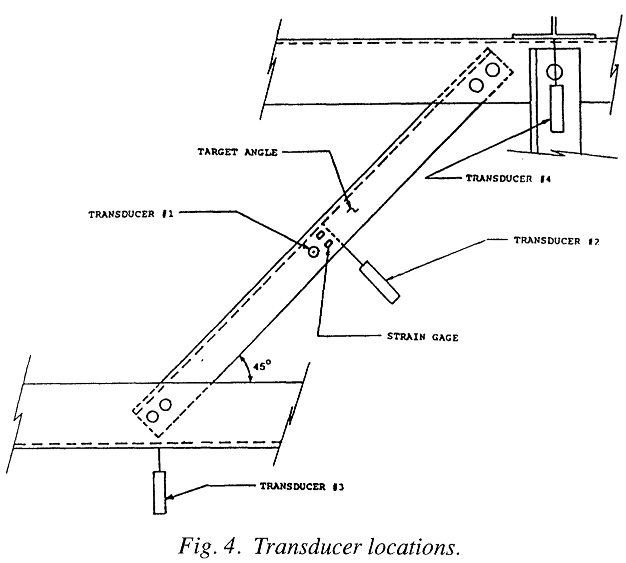

Fig. 4. Transducer locations.

either the geometric or the minor axis; the first will be classified as **LT** and the other two as **LG** and **LM**, respectively. Most of the local buckling occurred near the bolt hole. It is important to note that this could be due to the stress concentration at this location. Some local buckling, however, occurred away from the connection near the middle of the member. The photographs in Figs. 6 and 7 show **LT** and **LG** failures for specimens 10 and 47, respectively. The second failure mode is global buckling without any appreciable local buckling. This second failure mode can be divided into three

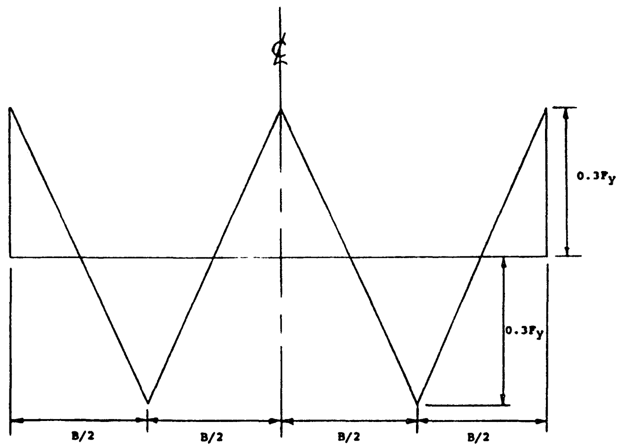

Fig. 5. Assumed residual stress distribution.

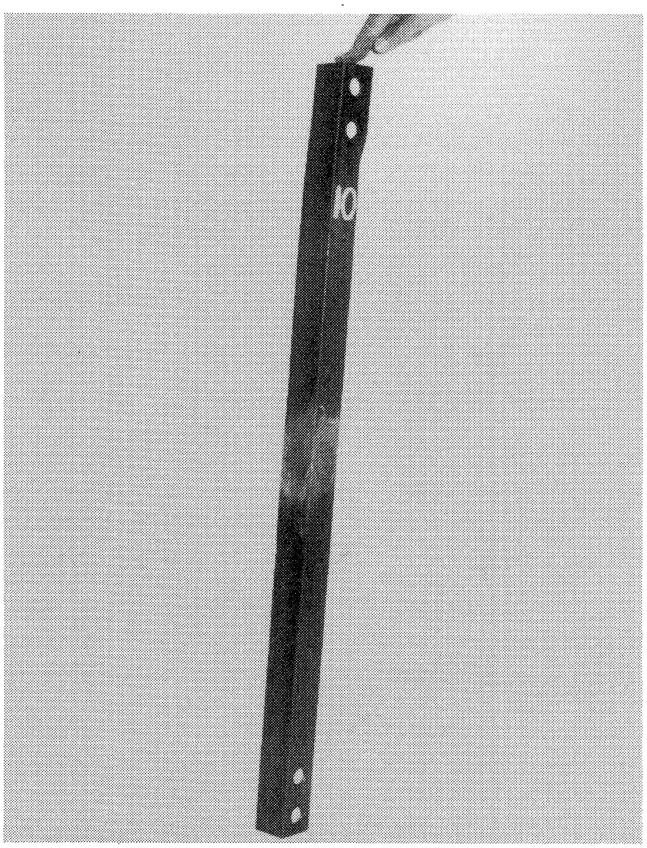

Fig. 6. LT failure—Specimen 10.

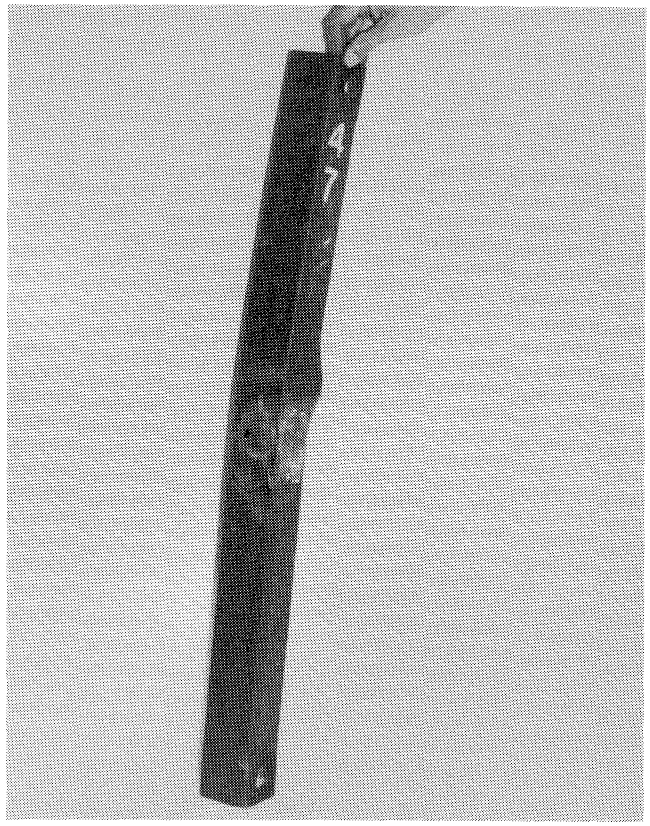

Fig. 7. LG failure—Specimen 47.

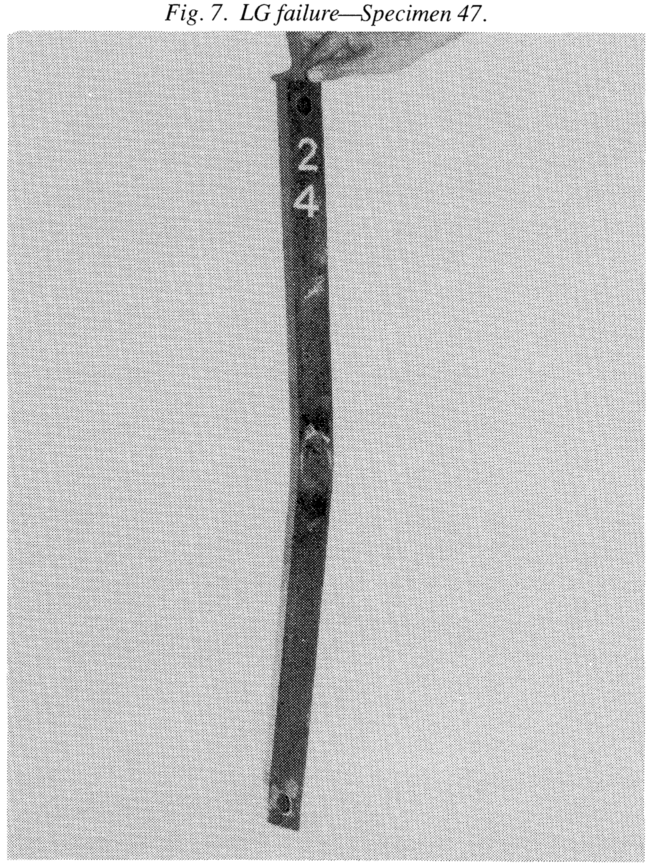

Fig. 8. FT failure—Specimen 24.

types of failure. The first is a minor axis flexural buckling failure (referred to as **FM**), the second is a geometric axis flexural buckling failure (referred to as **FG**), and the third is a minor axis flexural buckling coupled with torsional buckling (referred to as **FT**). The photograph shown in Fig. 8 shows **FT** failure for member 24. Member forces vs. displacement and vs. strain for two members are given in Figs. 9 and 10. Member 34 (Fig. 9) failed primarily in a global mode, while member 9 (Fig. 10) failed primarily due to local buckling of the angle leg.

Failure Loads: Tables 2 and 3 list the failure loads and modes for each individual test, and the actual dimensions and the yield stress for each specimen. The tables are organized in the order of the previously mentioned groups.

As can be noted from the tables, groups 1, 3, 5, 6, 8, and 10 failed basically in the local mode while groups 2, 4, 7, and 9 failed in the flexural global mode. The angle leg width/thickness ratios for the groups, which failed in the flexural global mode, meet the AISC requirements to exclude local leg buckling. There are variations in the failure loads within each group. These variations are within 5 to 14 percent above and 3 to 18 percent below the mean within each group, and are within the accuracy limit expected from the test results. For the purpose of analyzing the differences in failure loads between groups, a variable *n*, which is defined as the fraction of the yield stress which would exist over the entire cross-section if the failure load was applied concentrically, was calculated. This facilitates the accounting for the effect of variations in area and yield stress. Due to the torsional effects as well as the effect of the eccentricity of the load, the *n* values are lower than what they would be for concentrically loaded members without torsion.

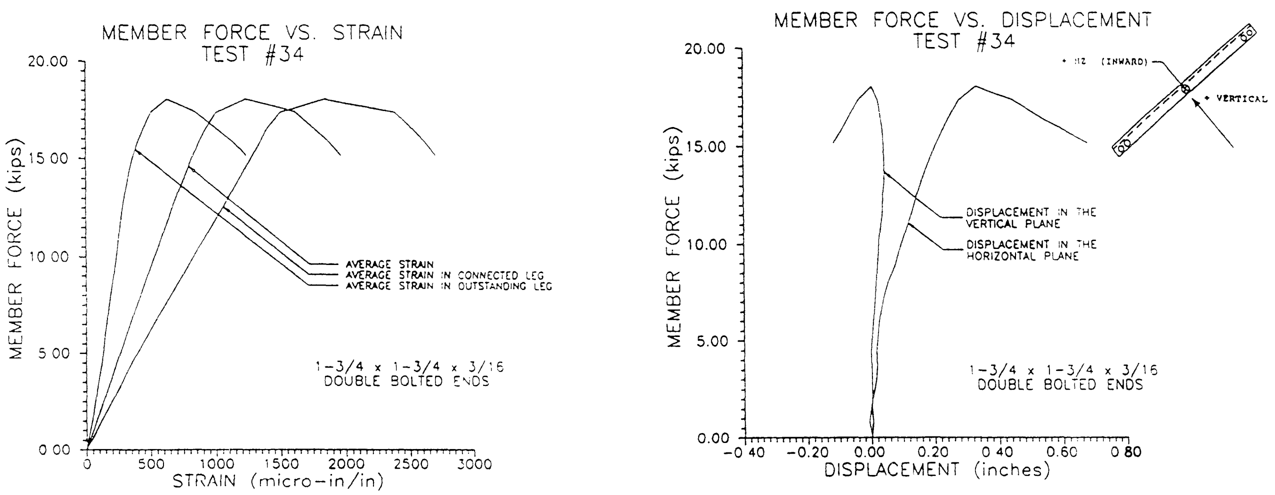

Fig. 9. Member force vs. strain and displacement Specimen 34.

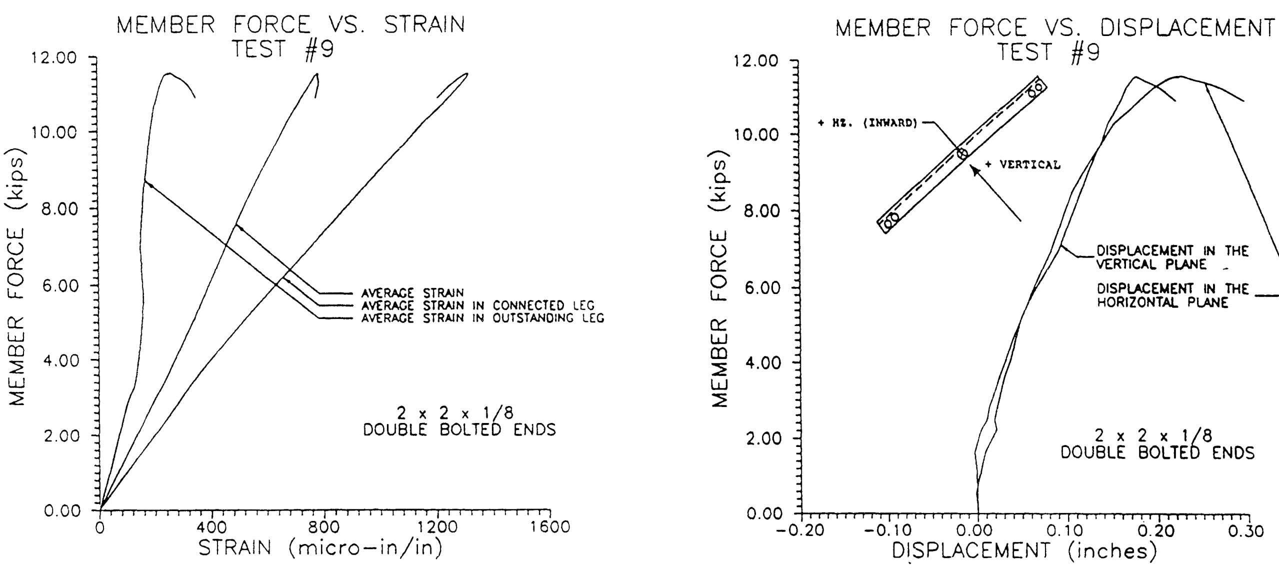

Fig. 10. Member force vs. strain and displacement Specimen 42.

Table 2. Tests Results for Double Bolted Specimens								
	Dimensions							
Test (1)	Width (in.) (2)	Thickness (in.) (3)	b/t (4)	F_y (ksi) (5)	$76\sqrt{F_y}$ (6)	Failure Mode (7)	Failure Load (kips) (8)	n* (9)
1	1.731	0.139	12.45	49.9	10.76	LG	11.07	0.480
2	1.720	0.141	12.20	52.7	10.47	LG	14.87	0.607
3	1.732	0.136	12.74	49.5	10.80	LM	14.30	0.638
4	1.733	0.140	12.38	50.0	10.75	LM	13.86	0.595
5	1.735	0.135	12.85	49.4	10.81	LG	13.08	0.588
6	1.762	0.199	8.85	47.6	11.02	FM	22.08	0.701
7	1.767	0.194	9.11	48.7	10.89	FM	21.81	0.691
8	1.767	0.198	8.92	47.7	11.00	FG	21.03	0.667
33	1.768	0.196	9.02	51.2	10.62	FM	19.22	0.573
34	1.794	0.197	9.11	49.7	10.78	FM	18.03	0.543
9	1.971	0.133	14.82	47.0	11.09	LT	11.55	0.485
10	1.973	0.131	15.06	46.4	11.16	LT	10.98	0.473
11	1.974	0.135	14.62	47.1	11.07	LT	14.50	0.598
12	2.016	0.131	15.39	49.7	10.78	LT	11.87	0.467
13	1.967	0.133	14.79	47.8	10.99	LT	14.50	0.600
20	1.992	0.200	9.96	47.4	11.04	FT	21.91	0.611
21	1.987	0.202	9.84	45.8	11.23	FT	19.85	0.569
22	1.985	0.195	10.18	47.6	11.02	FT	21.27	0.607
43	2.001	0.200	10.00	45.8	11.23	FT	19.08	0.548
44	2.008	0.198	10.17	45.5	11.27	FT	18.45	0.538
18	2.487	0.199	12.50	45.7	11.24	LT	25.33	0.583
19	2.483	0.199	12.48	47.5	11.03	LT	24.76	0.549
50	2.504	0.203	12.33	48.8	10.88	LT	26.50	0.557
51	2.508	0.200	12.54	47.5	11.03	LT	24.95	0.545
52	2.512	0.209	12.02	47.8	10.99	LT	26.10	0.543

Key to Failure Modes

LG: local buckling of the connected leg followed by flexural geometric axis buckling
LM: local buckling of the connected leg followed by flexural minor axis buckling
LT: local buckling of the connected leg followed by torsional buckling
FG: flexural geometric axis buckling
FM: flexural minor axis buckling
FT: flexural minor axis buckling coupled with torsional buckling

* $n = \dfrac{\text{Failure Load}}{F_y \times \text{Area}}$

NOTE: 1 in. = 25.4 mm   1 ksi = 6.895 MPa   1 kip = 4.448 kN

CURRENT DESIGN PRACTICE

In the United States, two documents address the design of single angle compression members; namely the AISC LRFD and ASD Specification for Structural Steel Buildings[1–3] and the ASCE Manual 52 for the Design of Steel Transmission Towers.[4] Both methods will be briefly described, and the results obtained by applying these methods will be compared with the test results.

ASCE MANUAL 52: The angle is always considered to be an axially loaded member; the end restraint effect (for slender members) and the load eccentricity (for non-slender members) are accounted for by the use of an effective slenderness ratio, (KL/r). The manual gives six formulas to calculate KL/r, three formulas are for non-slender members $L/r < 120$, namely for concentric loading at both ends, concentric loading at one end and eccentric at the other, and for eccentric loading at both ends. The other three formulas are for slender members $L/r > 120$, where elastic buckling prevails and rotational end restraint conditions control the design. One formula applies when the member is unrestrained against rotation at both ends, the second when the member is restrained at one end and unrestrained at the other, and the third applies when both ends are restrained. Local buckling

Test (1)	Dimensions: Width (in.) (2)	Dimensions: Thickness (in.) (3)	b/t (4)	F_y (ksi) (5)	$76\sqrt{F_y}$ (6)	Failure Mode (7)	Failure Load (kips) (8)	n* (9)
53	1.749	0.133	13.15	51.2	10.62	LT	10.80	0.471
54	1.747	0.132	13.23	49.5	10.80	LT	9.96	0.453
55	1.754	0.136	12.90	51.2	10.62	LT	10.07	0.429
56	1.749	0.135	12.96	51.0	10.64	LT	10.42	0.450
57	1.751	0.136	12.87	52.2	10.52	LT	9.89	0.414
23	test data inadequate—failure load not reached							
24	1.788	0.195	9.17	49.2	10.84	FT	15.16	0.467
35	1.769	0.202	8.76	49.3	10.82	FT	16.96	0.511
36	1.778	0.207	8.59	49.8	10.77	FT	17.49	0.507
37	1.776	0.190	9.35	50.4	10.71	FT	13.49	0.419
26	1.985	0.143	13.88	49.6	10.79	LT	10.26	0.378
27	1.976	0.138	14.32	48.1	10.96	LT	8.74	0.345
28	2.001	0.145	13.80	51.7	10.57	LT	9.53	0.330
38	1.967	0.139	14.15	50.8	10.66	LT	11.21	0.418
39	local failure affected strain readings—test data ignored							
29	test data inadequate—failure load not reached							
31	1.984	0.200	9.92	49.2	10.84	FT	19.33	0.521
40	1.998	0.196	10.19	46.8	11.11	FT	15.98	0.458
41	1.995	0.197	10.13	46.0	11.21	FT	18.22	0.530
42	1.998	0.190	10.52	46.1	11.19	FT	18.10	0.543
45	2.480	0.202	12.28	47.4	11.04	LT	19.64	0.431
46	2.501	0.203	12.32	48.1	10.96	LT	19.49	0.416
47	2.505	0.197	12.72	48.1	10.96	LG	20.19	0.443
48	2.498	0.194	12.88	47.7	11.00	LT	21.07	0.474
49	2.483	0.198	12.54	49.8	10.77	LT	19.94	0.424

Table 3. Tests Results for Single Bolted Specimens

Key to Failure Modes

LG: local buckling of the connected leg followed by flexural geometric axis buckling
LM: local buckling of the connected leg followed by flexural minor axis buckling
LT: local buckling of the connected leg followed by torsional buckling
FG: flexural geometric axis buckling
FM: flexural minor axis buckling
FT: flexural minor axis buckling coupled with torsional buckling

* $n = \dfrac{\text{Failure Load}}{F_y \times \text{Area}}$

NOTE: 1 in. = 25.4 mm   1 ksi = 6.895 MPa   1 kip = 4.448 kN

of the leg is considered by calculating a local buckling stress F_{cr}. Finally, the axial compressive stress F_a is calculated based on KL/r, F_{cr}, and the yield stress F_y.

AISC Specifications: Currently there are two versions of the AISC specification. One version is the Load Resistance Factor Design (LRFD), and the second is the Allowable Stress Design (ASD). The concepts of design of the concentrically loaded single-angle strut are basically the same in the LRFD and ASD specifications. An equivalent slenderness ratio is calculated taking the effect of the angle leg width/thickness ratio into consideration. The nominal axial load or the allowable axial stress is then calculated. The calculation is based on flexural and flexural-torsional buckling, and the smaller value is used.

Most single angle struts are eccentrically loaded and the effect of biaxial bending must be considered by using the appropriate interaction equation from Chapter H, in both the LRFD and ASD specifications. In the case of the LRFD Specification, when calculating the nominal bending moments, the limiting extreme fiber flexural stress is usually assumed to be equal to the yield stress. In the case of the ASD Specification the allowable bending stresses are calculated with due consideration of the member lateral stability.

Evaluation of the Design Methods: Both the AISC LRFD Specification, and Manual 52 are based on limit state design. Hence, the nominal loads without any reduction can be compared directly with the experimental failure loads. The test specimens nominal loads as predicted by the AISC LRFD

Table 4. AISC-LRFD Predicted Failure Loads for Double Bolted Specimens						
			Actual Failure	Manual 52	AISC-LRFD Failure Load	
Test (1)	b/t (2)	L/r (3)	Load (kips) (4)	Load (kips) (5)	$e = 0$* (kips) (6)	$e \neq 0$* (kips) (7)
1	12.45	98	11.07	10.90	11.03	5.32
2	12.20	98	14.87	10.78	11.17	5.47
3	12.74	98	14.30	10.76	10.77	5.22
4	12.38	98	13.86	11.07	11.15	5.38
5	12.85	98	13.08	10.75	10.72	5.18
6	8.85	99	22.08	15.90	16.04	7.02
7	9.11	99	21.81	15.89	15.90	7.04
8	8.92	99	21.03	15.90	16.09	7.03
33	9.02	99	19.22	15.67	16.31	7.28
34	9.11	99	18.03	16.39	16.84	7.41
9	14.82	85	11.55	13.38	13.31	6.24
10	15.06	85	10.98	13.13	13.02	6.13
11	14.62	85	14.50	13.53	13.60	6.36
12	15.39	85	11.87	13.62	13.87	6.61
13	14.79	85	14.50	13.24	13.36	6.29
20	9.96	86	21.91	20.01	21.27	8.99
21	9.84	86	19.85	19.91	21.00	8.74
22	10.18	86	21.27	19.34	20.67	8.78
43	10.00	86	19.08	20.09	21.12	8.79
44	10.17	86	18.45	19.96	21.00	8.75
18	12.50	67	25.33	28.42	30.72	12.66
19	12.48	67	24.76	28.38	31.31	12.96
50	12.33	67	26.50	29.53	32.65	13.60
51	12.54	67	24.95	28.73	31.71	13.25
52	12.02	67	26.10	30.23	33.20	13.74

NOTE: 1 in. = 25.4 mm 1 kip = 4.448 kN
**e* represents the eccentricity of the applied load

Specification (with and without the effect of the load eccentricity), and Manual 52 are given in Tables 4 and 5. In the same tables the experimental failure loads are given.

The predicted allowable loads for the test specimens (with and without the effect of the load eccentricity) based on the AISC ASD Specification are given in Tables 6 and 7. In the same tables the actual failure loads and the corresponding factors of safety (Failure Load/Allowable Load) are given.

As can be noted from Tables 4 and 5, the nominal loads calculated from Manual 52 are very close to or exceed the actual failure loads. A similar conclusion can be reached by examining the AISC LRFD Specification nominal loads for the concentrically loaded struts. When the eccentricity of the applied loads is taken into consideration, the AISC LRFD Specification nominal loads are very conservative. As can be noted from Tables 6 and 7, the safety factors are generally low if one ignores the effect of the load eccentricity. However, they are high if the effect of the load eccentricity is taken into consideration in the manner described earlier.

One possible way to resolve the overdesign in the AISC specifications is to consider the end restraint effect by using an effective length factor less than one. Another issue, which can be resolved more easily to get rid of the conservatism, is not to add the worst case bending stresses due to load eccentricities that do not occur at the same point of the angle cross section as suggested in the AISC Manual. It is more correct to combine the axial and bending stresses at the angle tips and heel and then to use the interaction equation to determine the allowable load based on the most critical point.

SUMMARY AND CONCLUSIONS

In this paper a test program for non-slender single angle members with equal legs, utilizing a three-dimensional truss, was briefly described. The test results were given and ana-

Table 5. AISC-LRFD Predicted Failure Loads for Single Bolted Specimens						
			Actual Failure Load	Manual 52 Load	AISC-LRFD Failure Load	
Test (1)	b/t (2)	L/r (3)	(kips) (4)	(kips) (5)	$e = 0$* (kips) (6)	$e \neq 0$* (kips) (7)
53	13.15	92	10.80	11.35	11.70	5.56
54	13.23	92	9.96	11.25	11.44	5.42
55	12.90	92	10.07	11.62	12.06	5.70
56	12.96	92	10.42	11.62	11.88	5.62
57	12.87	92	9.89	11.64	12.09	5.75
23	test data inadequate—failure load not reached					
24	9.17	93	15.16	16.90	17.82	7.62
35	8.76	93	16.96	17.02	17.97	7.61
36	8.59	93	17.49	17.57	18.67	7.91
37	9.35	93	13.49	16.30	17.30	7.50
26	13.88	80	10.26	15.15	15.57	7.17
27	14.32	80	8.74	14.46	14.90	6.84
28	13.80	80	9.53	15.76	15.97	7.52
38	14.15	80	11.21	14.59	15.27	7.08
39	local failure affected strain readings					
29	test data inadequate—failure load not reached					
31	9.92	81	19.33	20.83	22.84	9.43
40	10.19	81	15.98	20.49	22.14	9.07
41	10.13	81	18.22	20.34	21.97	9.01
42	10.52	81	18.10	19.67	21.33	8.81
45	12.28	65	19.64	29.38	32.16	13.28
46	12.32	65	19.49	30.12	32.57	13.57
47	12.72	65	20.19	29.29	31.61	13.29
48	12.88	65	21.07	28.61	30.99	13.04
49	12.54	65	19.94	28.99	32.39	13.61

NOTE: 1 in. = 25.4 mm 1 kip = 4.448 kN
*e represents the eccentricity of the applied load

lyzed. Comparisons were made between the actual failure loads and those predicted using methods given in the ASCE Manual 52 for Steel Transmission Towers and the AISC Specification for Steel Buildings. The test results reported in this paper indicate that current design methods for nonslender single angle members are not adequate.

ACKNOWLEDGMENTS

This study was partially funded by Bonneville Power Administration and Ontario Hydro. Funds were received from the University of Maine in the form of release time for the first two authors and graduate assistantship for the third author. Maine Cascade Iron Works of Clinton, ME supplied the testing truss as a donation to the University of Maine.

REFERENCES

1. *Load and Resistance Factor Design Specification for Structural Steel Buildings*, AISC, 1986.
2. *Specification for Structural Steel Buildings, Allowable Stress Design and Plastic Design,* AISC, 1989.
3. *Specification for Allowable Stress Design of Single-Angle Members, AISC Manual of Steel Construction,* 9th ed., 1989.
4. *ASCE Manual 52, Guide for Design of Steel Transmission Towers,* 2nd ed., 1988.

Table 6.
AISC Allowable Stress Predicted Failure Loads for Double Bolted Specimens

Test (1)	Failure Load (kips) (2)	$e = 0$*		$e \neq 0$*	
		R_a (kips) (3)	Safety Factor (4)	R_a (kips) (5)	Safety Factor (6)
1	11.07	6.76	1.64	2.91	3.80
2	14.87	6.83	2.18	2.99	4.97
3	14.30	6.60	2.17	2.84	5.04
4	13.86	6.83	2.03	2.94	4.71
5	13.08	6.57	1.99	2.83	4.62
6	22.08	9.83	2.25	3.93	5.62
7	21.81	9.74	2.24	3.92	5.56
8	21.03	9.86	2.13	3.94	5.34
33	19.22	9.98	1.93	4.07	4.72
34	18.03	10.32	1.75	4.16	4.33
9	11.55	8.08	1.43	3.30	3.50
10	10.98	7.89	1.39	3.22	3.41
11	14.50	8.26	1.76	3.37	4.30
12	11.87	8.41	1.41	3.43	3.46
13	14.50	8.11	1.79	3.31	4.38
20	21.91	12.98	1.69	5.01	4.37
21	19.85	12.80	1.55	4.87	4.08
22	21.27	12.61	1.69	4.91	4.33
43	19.08	12.86	1.48	4.93	3.87
44	18.45	12.78	1.44	4.90	3.77
18	25.33	18.28	1.39	6.86	3.69
19	24.76	18.66	1.33	7.00	3.54
50	26.50	19.44	1.36	7.35	3.61
51	24.95	18.85	1.32	7.13	3.50
52	26.10	20.20	1.29	7.52	3.47

*e represents the eccentricity of the applied load

Table 7. AISC Allowable Stress Predicted Failure Loads for SIngle Bolted Specimens

Test (1)	Failure Load (kips) (2)	$e = 0$* R_a (kips) (3)	$e = 0$* Safety Factor (4)	$e \neq 0$* R_a (kips) (5)	$e \neq 0$* Safety Factor (6)
53	10.80	7.16	1.51	3.00	3.60
54	9.96	7.00	1.42	2.92	3.41
55	10.07	7.39	1.36	3.08	3.27
56	10.42	7.28	1.43	3.05	3.42
57	9.89	7.41	1.33	3.10	3.19
23	test data inadequate				
24	15.16	10.92	1.39	4.25	3.57
35	16.96	11.02	1.54	4.25	3.99
36	17.49	11.44	1.53	4.42	3.96
37	13.49	10.60	1.27	4.18	3.23
26	10.26	9.41	1.09	3.82	2.69
27	8.74	8.98	0.97	3.59	2.43
28	9.53	9.68	0.98	3.98	2.39
38	11.21	9.25	1.21	3.72	3.01
39	test data inadequate				
29	test data inadequate				
31	19.33	13.89	1.39	5.29	3.65
40	15.98	13.42	1.19	5.07	3.15
41	18.22	13.31	1.37	4.99	3.65
42	18.10	12.92	1.40	4.89	3.70
45	19.64	19.09	1.03	7.21	2.72
46	19.49	19.36	1.01	7.37	2.64
47	20.19	18.76	1.08	7.14	2.83
48	21.07	18.37	1.15	6.99	3.01
49	19.94	19.24	1.04	7.27	2.74

*e represents the eccentricity of the applied load